Mon. Not. R. Astron. Soc. **000**, 1–7 (2006) Printed 12 August 2008 (MN LaTeX style file v2.2)

A low mass cluster of extremely red galaxies at z=1.10 in the GOODS Southern Field

Anastasio Díaz–Sánchez[1⋆], Isidro Villo–Pérez[2], Antonio Pérez–Garrido[1] and Rafael Rebolo[3,4]

[1] *Dpto. Física Aplicada, Universidad Politécnica de Cartagena, Campus Muralla del Mar, 30202 Cartagena, Murcia, Spain*
[2] *Dpto. Electrónica, Tecnología de Computadores y Proyectos, Universidad Politécnica de Cartagena, Campus Muralla del Mar, 30202 Cartagena, Murcia, Spain*
[3] *Instituto de Astrofísica de Canarias, Vía Láctea s/n, 38200 La Laguna, Tenerife, Spain*
[4] *Consejo Superior de Investigaciones Científicas, Spain*

arXiv:astro-ph/0702523v1 20 Feb 2007

12 August 2008

ABSTRACT

We have studied the spatial clustering of high redshift ($z > 1$) extremely red objects (EROs) as a function of photometric redshift in the GOODS Southern Field using public data. A remarkable overdensity of extremely red galaxies ($I - K_s > 4$) is found at an average photometric redshift $z_{\rm phot} = 1.10$. Nine objects (six are EROs) within 50 arcsec of the brightest infrared galaxy in this overdensity present spectroscopic redshifts in the range $1.094 < z_{\rm spec} < 1.101$ with a line-of-sight velocity dispersion of $\sigma_v = 433^{+152}_{-74}$ km s^{-1} typical of an Abell richness class $R = 0$ cluster. Other potential members of this cluster, designated as GCL J0332.2-2752, have been identified using photometric redshifts and the galaxy density profile studied as a function of radius. The mass of the cluster is preliminary estimated at $M_{cl} \sim 5 - 7 \times 10^{13} M_{\odot}$. Using available Chandra data, we limit the rest-frame X-ray luminosity of the cluster to less than $L_X = 7.3 \times 10^{42}$ erg s^{-1} (0.5-2.0 keV). This low-mass, low L_X cluster at $z > 1$ shows the potential of EROs to trace clusters of galaxies at high redshift.

Key words: galaxies: clusters: general — galaxies: evolution — galaxies: high-redshift — large-scale structure of Universe

1 INTRODUCTION

Clusters of galaxies trace the largest gravitationally bound mass concentrations in the Universe. The number density of galaxy clusters as a function of mass and redshift provide a testbed for cosmological models and set constraints on cosmological parameters such as the density of dark matter and the equation of state of dark energy (Capozziello & Cardone 2004; Munshi et al. 2004). Clusters at various redshifts also provide samples of galaxies in dense environments to confront galaxy formation and evolution theories.

Optical and near infrared follow-up of X-ray sources is a proven technique for constructing large samples of distant clusters (Rosati, et al. 2002a), however it has provided only about ten clusters with X-ray emission confirmed at $z > 1$, the highest redshift cluster being at $z = 1.41 - 1.45$ (Mullis et al. 2005; Stanford et al. 2006). The majority of the other confirmed clusters at $z > 1$ have been identified in photometric surveys around radio-sources (Blanton et al. 2003; Best 2000; Nakata et al. 2001).

High-redshift low X-ray luminosity (low-T) clusters are often below the limit of X-ray surveys. Deep infrared surveys offer an alternative path to identify high redshift galaxy clusters. The cores of these clusters are expected to be dominated by elliptical galaxies which at $z > 1$ appear as extremely red objects (EROs) with colours $I - K > 4$. A significant fraction of these red objects ($30 - 45\%$ of the total number at $K_s = 20 - 22$ in the general field) are early-type galaxies and have redshift distributions with $z_{\rm mean} \approx 1.2$ (Moustakas et al. 2004; Stanford et al. 1997). Several spectroscopic studies have shown the EROs population is heterogeneous, being mainly formed by old passively evolving distant elliptical galaxies and extremely dust reddened starburst galaxies (Cimatti et al. 2002, 2003). EROs have strong spatial clustering, comparable to that of present-day luminous ellipticals, which has been interpreted as evidence that distant EROs and nearby ellipticals are evolutionary linked, i. e., EROs could be the progenitors of present day massive elliptical galaxies. At least two distant clusters of EROs have been confirmed in general field surveys at $z = 1.27$

⋆ E-mail: andiaz@upct.es

(Stanford et al. 1997) and $z = 1.41$ (Stanford et al. 2005), respectively.

In this paper we study the clustering of high redshift ($z > 1$) EROS as a function of photometric redshift in the GOODS Southern field and report on a cluster of galaxies at $z = 1.10$ with at least ten spectroscopically confirmed members within a 92 arcsec radius region. The use of public data, catalogues, and the cluster-finding algorithm are described in Section 2. The basic properties of this galaxy cluster are described in Section 3 and conclusions are given in Section 4. We assume a standard concordance cosmological model throughout, with $H_0 = 70$ km s^{-1} Mpc^{-1}, $\Omega_m = 0.3$, and $\Omega_\Lambda = 0.7$.

2 SAMPLE AND CLUSTER-FINDING ALGORITHM

We have studied the spatial distribution of EROS (defined here as objects with $i - K_s > 4$). in the GOODS-MUSIC (MUltiwavelength Southern Infrared Catalogue) dataset (Grazian et al. 2006) as a method to identify clusters of galaxies at high redshift. The GOODS-MUSIC catalogue includes the $F435W$ (B), $F606W$ (V), $F775W$ (i), and $F850LP$ (z) ACS data, the JHK_s VLT-ISAAC data, the Spitzer data provided by IRAC, and the available U-band data from 2.2ESO and VLT-VIMOS. The images from space and ground-based telescopes are of different resolution and depth and the colours are PSF matched. In this work we use the Vega system while in the GOODS-MUSIC catalogue magnitudes are given in the AB system. The ACS data and the VLT-ISAAC data were converted to the Vega system using $(B, V, i, z, J, H, K_s)_{\rm Vega} = (B, V, i, z, J, H, K_s)_{\rm AB} + (0.106, -0.088, -0.398, -0.536, -0.90, -1.38, -1.86)$ [1]. The catalogue is complete at $i_{\rm comp} = 26.1$ and $K_{s,\rm comp} = 22$ (Vega scale) (Grazian et al. 2006) and lists photometric redshifts $z_{\rm phot}$ for all the objects with average uncertainty $\sigma_{\rm phot} = 0.06$.

The spectroscopic catalogues used by GOODS-MUSIC are the COMBO-17 survey (Wolf et al. 2001), the CXO-CDFS survey (Szokoly et al. 2004), the K20 survey (Mignoli et al. 2005), the GOODS V1.0 survey (Vanzella et al. 2005), the VVDS survey (LeFevre et al. 2004) and the MASTER catalogue [2]. Spectroscopic redshift $z_{\rm spec}$ are available for more than 1000 objects. We will also work with the GOODS V2.0 survey (Vanzella et al. 2006). As early-type galaxies with $1 \leqslant z \leqslant 2$ have their rest-frame light peaks at the near-infrared band we only consider galaxies whith $K_s \leqslant K_{s,\rm comp}$, where $K_{s,\rm comp}$ is the completeness limit of the catalogue.

A simple cluster-finding algorithm was implemented to search for overdensities of EROs in the GOODS-MUSIC dataset with redshift in the range $1 < z_{\rm phot} < 2$. We adopted 0.8 Mpc as the radius of the circles used in the density determination (~ 1.6 arcmin for $1 < z < 2$ according to the concordance cosmological model). This is smaller than the Abell radius of a typical cluster $r_{\rm Abell} \sim 1.5$ Mpc but we expected that EROs mostly concentrate in the core of the clusters.

To detect spatial clustering at a given redshift z we first selected the total sample of EROs in the catalogue with $z_{\rm phot}$ within the interval $[z - \sigma_{\rm phot} z; z + \sigma_{\rm phot} z]$, where $\sigma_{\rm phot}$ is the average uncertainty of photometric redshifts. The density of EROs was then computed in circles of radius ~ 1.6 arcmin centred around each ERO of the sample, and this value was compared with the density of EROs in the whole GOODS Southern survey (~ 140 arcmin^2) at the given redshift. Only overdensities a factor 3 higher than the average were considered as potential galaxy clusters, provided the objects also followed a galactic red sequence in the $i - K_s$ vs. K_s diagramme. The redshift of the candidate cluster $z_{\rm cl}$ was then preliminary adopted as the average value of the photometric redshifts of the EROs in the overdensity.

We found four ERO overdensities with main properties listed in Table 1. For each potential cluster we checked the availability of spectroscopic redshifts. The overdensity at $z_{\rm cl} = 1.00$ contains four objects with spectroscopic redshift z_{spec} but they lie in an interval $\Delta z_{spec} = z_{max} - z_{min} = 0.08$ which is too wide for a cluster of galaxies. For the second overdensity listed in Table 1, we find 10 EROs with spectroscopic redshifts within the indicated redshift interval, six lie in a $\Delta z_{spec} = 0.004$ interval around $z_{\rm mean} = 1.098$, confirming that this region contains an excellent galaxy cluster candidate. Of the remaining four objects, two are at $z = 1.12$ and the other at $z = 1.044$ making unplausible a physical relation to the galaxy cluster. We note that the two remaining higher redshift candidate overdensities in Table 1 are less reliable given the wide redshift interval under consideration. Unfortunately, there is insufficient spectroscopic information and we shall await for additional data before making any further consideration on these potentially interesting overdensities.

3 THE GCL J0332.2-2752 CLUSTER OF GALAXIES AT $Z = 1.10$

We now concentrate on the EROs overdensity at $z_{\rm cl} = 1.10$. In Table 2 we list identification numbers, coordinates, redshifts, spectroscopic class, spectroscopic catalogue, K_s magnitude and $i - K_s$ colour for ten galaxies in this region with spectroscopic redshifts in the range $1.094 < z_{\rm spec} < 1.103$. From these ten galaxies we obtain a mean spectroscopic redshift for the cluster $< z >= 1.0986$ and a rms dispersion $\sigma = 0.0028$. We tentatively determine the equatorial coordinates of the cluster centre as the centroid of the coordinates for the six EROs in Table 2, which are $\alpha_{J2000.0} = 03^h 32^m 17.5^s$, $\delta_{J2000.0} = -27^\circ 52^m 32^s$. Hereinafter we will refer to this cluster as GCl J0332.2-2752. In Fig. 1 we plot a BVz false-colour image, from the ACS images, of the region showing the location of nine of these objects within 50 arcsec of the brightest infrared galaxy at z=1.098 which is close to the centre of the cluster. Six of them are EROs (marked in red in the figure) and lie within a radius of 24 arcsec from this galaxy. The other four are no-ERO galaxies, three appear in the figure marked with yellow open circles. The galaxy ID 2859 with the highest redshift ($z_{\rm spec} = 1.103$) is also at the largest angular distance 92 arcsec of the central region of the cluster and it

[1] http://www.eso.org/science/goods/release/20050930/ and http://www.stsci.edu/hst/acs/analysis/zeropoints/

[2] http://www.eso.org/science/goods/spectroscopy/CDFS_Mastercat/

Table 1. ERO overdensities at $1 < z_{\rm phot} < 2$.

$z_{\rm cl}$	Photometric redshift interval	Number of EROs	EROs with measured z_{spec}	Overdensity factor	Total ERO density [a] (galaxies/arcmin^2)	RA [b] J2000	Dec [c] J2000
1.00	0.940–1.060	10	4	3.78	0.33	53.09576	-27.87832
1.10	1.034–1.166	17	10	4.11	0.51	53.08198	-27.88069
1.70	1.598–1.802	15	1	3.10	0.60	53.11302	-27.71836
1.95	1.833–2.067	13	0	3.10	0.52	53.06804	-27.83184

[a] Density of EROs with $z_{\rm phot}$ within the photometric redshift interval in the whole GOODS-MUSIC dataset.
[b] Right ascension of the centroid of the coordinates for the EROs, in decimal degrees (J2000).
[c] Declination of the centroid of the coordinates for the EROs, in decimal degrees (J2000).

Table 2. Spectroscopic candidates of the GCl J0332.2-2752 cluster of galaxies at $z = 1.10$.

ID	RA [a] J2000	Dec [b] J2000	z [c]	qz [d]	class [e]	catalogue [f]	K_s	$i - K_s$
2859	53.09842	-27.88740	1.103	0	EMISSION	GOODSV2.0	21.83	2.35 ±0.10
3185	53.06122	-27.88284	1.101	0	EMISSION	GOODSV2.0	21.22	2.38 ±0.05
3315	53.07283	-27.88000	1.095	0	EARLY	GOODSV2.0	18.06	4.41 ±0.04
3490	53.06739	-27.87814	1.094	1	EARLY	GOODSV2.0	19.04	4.18 ±0.06
3586	53.06193	-27.87676	1.101	1	GALAXY	VVDS	20.05	2.67 ±0.04
3619	53.07276	-27.87632	1.100	0	EARLY	GOODSV2.0	18.21	4.25 ±0.04
3656	53.06210	-27.87654	1.101	2	GALAXY	MASTER	22.19	2.27 ±0.10
3698	53.07340	-27.87458	1.098	0	COMPOSITE	GOODSV2.0	17.52	3.99 ±0.02
3920	53.07155	-27.87245	1.097	0	AGN	CXO-CDFS	18.07	4.18 ±0.04
3941	53.08044	-27.87204	1.096	0	EARLY	GOODSV2.0	18.12	4.60 ±0.07

[a] Right ascension, in decimal degrees (J2000).
[b] Declination, in decimal degrees (J2000).
[c] Spectroscopic redshift.
[d] Quality of spectroscopic redshift (0 = very good, 1 = good, 2 = uncertain, 3 = bad quality).
[e] Spectroscopic class (Grazian et al. 2006).
[f] Reference spectroscopic catalogue.

is not shown in the image. We also note the presence of an AGN ($z = 1.097$) of type QSO-2 near the central region (Szokoly et al. 2004). The nine galaxies in the image are classified as follows: six are EROs, out of which four belong to the "early" class, the most luminous galaxy is a "composite" (early+late type galaxy) class and one is an AGN. Out of the three no-EROs, two belong to the class "galaxy" (this means that there is no information in the catalogue about what type of galaxy it is) and the other to "emission" class, as defined by Grazian et al. (2006).

We now estimate the velocity dispersion of the GCl J0332.2-2752 along the line-of-sight from the ten galaxy members with available spectroscopic redshifts obtaining $\sigma_v = 433^{+152}_{-74}$ km s^{-1}, with the 68% confidence uncertainty estimated according to the expression given by Danese et al. (1980). This velocity dispersion corresponds to the median value for Abell richness class $R = 0$ (Yee & Ellingson 2003). In order to estimate the mass and the size of the cluster we calculate the radius R_{200}, which approximates the virial radius. It is the radius inside which the density is 200 times the critical density, $200\rho_c(z) = M_{\rm cl}/(4\pi/3)R_{200}^3$. Using the redshift dependence of the critical density and the virial mass, $M_{\rm cl} = 3\sigma_v^2 R_{200}/G$, we obtain (Finn et al. 2005):

$$R_{200} = 2.47 \frac{\sigma_v}{1000 \text{ km s}^{-1}} \frac{1}{\sqrt{\Omega_m(1+z)^3 + \Omega_\Lambda}} \text{ Mpc} . \quad (1)$$

For the cluster GCl J0332.2-2752 we have $R_{200} = 0.57^{+0.2}_{-0.1}$ Mpc or $R_{200} = 69^{+24}_{-11}$ arcsec. We combine the virial mass with the expression for R_{200} to obtain an estimate of the cluster mass in terms of σ_v and cosmological parameters:

$$M_{\rm cl} = 1.71\times10^{15} \left(\frac{\sigma_v}{1000 \text{ km s}^{-1}}\right)^3 \frac{1}{\sqrt{\Omega_m(1+z)^3 + \Omega_\Lambda}} M_\odot , \quad (2)$$

which gives a mass for our cluster $M_{\rm cl} = 7^{+2}_{-1}\times10^{13} M_\odot$. If we use the more empirical $M_{200}-\sigma_v$ relation given by expression 47 in Voit (2005) we have $M_{\rm cl} = 4.9^{+1.6}_{-0.8} \times 10^{13} M_\odot$. If the intracluster gas shares the same dynamics of typical galaxy clusters its temperature T can be estimated from $k_B T \simeq \mu m_p \sigma_v^2 \simeq 6 \frac{\sigma_v^2}{10^6 (\text{km s}^{-1})^2}$ keV (Rosati, et al. 2002a), where μ is the mean molecular weight ($\mu \sim 0.6$ for a primordial contribution with a 76% fraction contributed by hydrogen) and m_p is the proton mass. We estimate $k_B T \simeq 1.1^{+0.8}_{-0.4}$ keV. This compares well with the value, $k_B T \simeq 1.5 \pm 0.6$ keV, inferred from the σ_v-T prescriptions by Lubin et al. (1993).

A comparison of photometric and spectroscopic red-

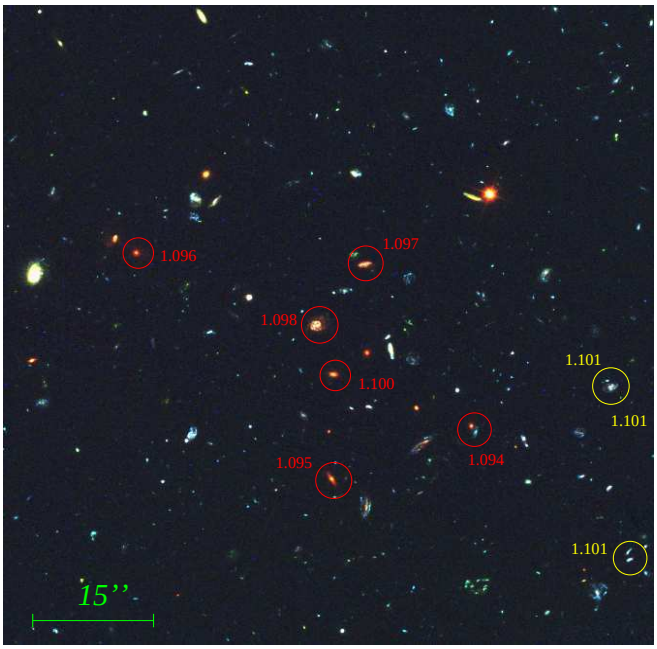

Figure 1. BVz false-colour ACS (Hubble) image of the GCl J0332.2-2752 cluster of galaxies covering 1.36 arcmin on a side. The EROs members of the cluster with measured spectroscopic redshift are marked with red open circles and their $z_{\rm spec}$ are given by red numbers. The no-ERO members with measured spectroscopic redshift are marked with yellow open circles and their $z_{\rm spec}$ are given by yellow numbers. The galaxy with $z = 1.098$ is the most luminous, the AGN with $z = 1.097$ is of type QSO-2. The double redshift label for one circle indicates independent redshifts for two close galaxies. North is up and East is left.

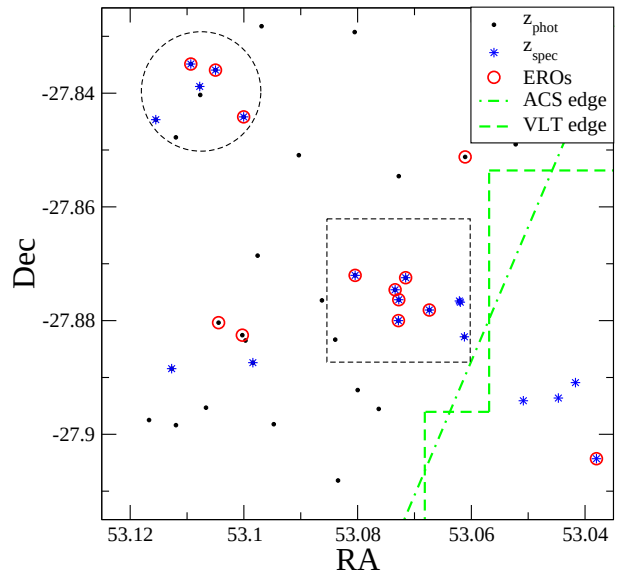

Figure 2. Distribution of galaxies with $z_{\rm phot}$ within the interval $[1.088; 1.107]$ in the region of GCl J0332.2-2752 . The edges of the ACS images and VLT-ISAAC images are shown. Photometric candidates are marked by dots, galaxies with measured $z_{\rm spec}$ are marked by blue stars and EROs are also marked by red open circles. The field of Fig 1 is also shown as a dashed box. A group of galaxies is shown within the dashed circle. There are also four galaxies in the bottom-right part, which are outside of the GOODS-MUSIC area, with measured spectroscopic redshift.

shifts for objects around z=1.1 in the GOODS-MUSIC sample shows little scatter suggesting that the uncertainties of the photometric redshifts are lower than 1 %. This implies that new cluster members can be reliably identified using photometric redshifts. In Fig. 2 we plot the spatial distribution of galaxies with redshifts $1.088 < z < 1.107$ ($< z > \pm 3\sigma$) in a wider region of the sky. Both, objects with spectroscopic and photometric redshift determinations are plotted. A number of potential cluster members are found in the immediate vicinity of the region that contains the higher ERO overdensity. A colour-magnitude diagram, $i - K_s$ vs. K_s of galaxies within a radius of 1.6 arcmin of the cluster centre is shown in Fig. 3. We can see that the most luminous EROs follow a well defined red sequence, as expected. We also find at fainter magnitudes K_s >20 a possible sequence of galaxies with average colour $i - K_s = 2.5$. It appears that both sequences are similarly populated and that the fainter one is mostly due to spiral galaxies (Butcher & Oemler 1984; Tomotsugu et al. 2003). Following Hansen et al. (2005) we can estimate the richness for the cluster as the number of galaxies in the upper red sequence, we find here $N_{\rm gal_r} = 8$. Low redshift galaxy clusters with this value show velocity dispersions which are similar (Hansen et al. 2005) within error bars to the one measured for GCl J0332.2-2752.

In Fig. 4 we give the galaxy density profile of the cluster as a function of radius, here we consider galaxies with $z_{\rm phot}$ within the interval $[1.088; 1.107]$. We evaluate the density profile taking annuli centred at the optical centre of the cluster, when the radius arrives to the edge of the field images ($\sim$ 55 arcsec) we take semiannuli in the direction away from the edges (east direction). The dashed line in Fig. 4 left is a fit with a power law $\Sigma = N_0 r^{-\alpha}$ with exponent $\alpha = 1.0 \pm 0.1$ and $N_0 = 0.04 \pm 0.01$, which agrees with the behaviour found in low redshift clusters (Hansen et al. 2005). We now fit the density profile with a NFW model (Navarro et al. 1993), where the 3D number density profile is $n(x) = n_0 x^{-1}(1+x)^{-2}$ with n_0 the normalisation and $x = r/r_s$, where r_s is a scale radius. The r_s scale radius is related by $r_s \equiv R_{200}/c_g$ to the virial radius R_{200} and the galaxy concentration parameter c_g. The surface density is then an integral of the 3D profile $\Sigma(x) = 2 n_0 r_s \int_0^{2/\pi} \cos\theta (\cos\theta + x)^{-2} d\theta$ (Baltermann et al. 1996). Using $R_{200} = 0.69$ arcsec we fit the data in the right panel of Fig. 4 to obtain $n_0 = 0.11 \pm 0.02$ galaxies/arcsec^2 and $c_g = 15 \pm 4$. The galaxy concentration parameter is higher than those found for low redshift clusters $c_g \sim 2 - 7$ (Hansen et al. 2005; Pointecouteau et al. 2005) and in simulations $c_g \sim 2 - 10$ (Jing 2000). The excess of galaxies that can be noticed at $r/R_{200} = 2.45$ in the right panel of Fig. 4 corresponds to a group of galaxies located at the top of Fig. 2 (dashed circle). There are spectroscopic redshifts for five of these galaxies (of which 3 are EROs). The mean

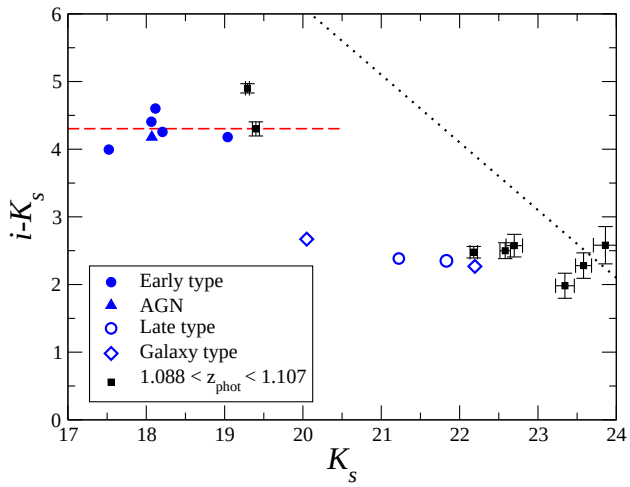

Figure 3. Colour-magnitude diagram for the candidates to the GCl J0332.2-2752 cluster of galaxies with $z_{\rm phot}$ within the interval [1.088; 1.107]. The members of the clusters with measured $z_{\rm spec}$ are marked by blue colours and their errors are equal or smaller than the sizes of the symbols. The red dashed line is the mean value of the $i-K_s$ colour for the EROs and the dotted line is the completeness i-band limit. Colours are PSF matched between the ACS and ISAAC magnitudes and they are in the Vega system.

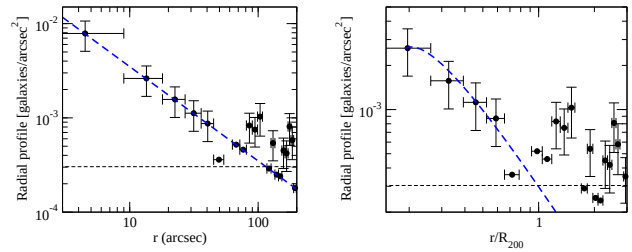

Figure 4. The galaxy density profile as a function of the radius for the GCl J0332.2-2752 cluster of galaxies, here we consider galaxies with $z_{\rm phot}$ within the interval [1.088; 1.107]. The black dashed lines in both figures are the mean density of galaxies within the interval [1.088; 1.107] in the whole GOODS-MUSIC area which is 0.000303 galaxies/arcsec^2. Left: the blue dashed line is a fit of a power law $\Sigma = N_0 r^{-\alpha}$ with exponent $\alpha = 1.0 \pm 0.1$ and $N_0 = 0.04 \pm 0.01$. Right: the galaxy density profile as a function of the radius divided by R_{200} for the GCl J0332.2-2752 cluster of galaxies. The best-fitting NFW profile is shown by the blue dashed line.

redshift of the group is $< z >= 1.0964$, remarkably similar to that of GCl J0332.2-2752 and the rms dispersion is $\sigma = 0.0020$. The centroid of this group in equatorial coordinates is $\alpha_{J2000.0} = 03^h32^m25.8^s$, $\delta_{J2000.0} = -27^\circ 50^m22^s$, thus it is located at an angular distance of 169 arcsec (1.41 Mpc) from the cluster. It is then plausible that both systems of galaxies form part or will become part of the same cluster. There are also four galaxies in the bottom-right part of Fig. 2, which are outside of the GOODS-MUSIC area, with spectroscopic redshift measured in LeFevre et al. (2004). The mean redshift of these galaxies is $< z >= 1.099$ and the rms dispersion is $\sigma = 0.0018$, the nearest galaxy to the centre of GCl J0332.2-2752 is at 102 arcsec (0.84 Mpc) and the farthest is an ERO at 156 arcsec (1.28 Mpc). It is unfortunate that the location of GCl J0332.2-2752 near the edge of the GOODS field prevents identification of other potential substructures. According to hierarchical structure formation it is plausible that distant clusters may be conformed by smaller substructures with rather cool gas, e.g. Frenk et al. (1996). In the Chandra Deep Field South (CDF-S) there is evidence for sheets in the distribution of galaxies at $z = 0.666$, $z = 0.734$, $z = 1.096$, $z = 1.221$, $z = 1.300$ and $z = 1.614$ (Vanzella et al. 2006). Two X-ray clusters have been identified in correspondence with the spikes in the redshift distribution at $z = 0.666$, $z = 0.734$ (Giacconi et al. 2002; Gilli 2004), these clusters are knots of sheet-like structures extending over several Mpc. Using a friend-of-friend algorithm, Adami et al. (2005) also identified a compact structure of galaxies called "Structure 15" at z=1.098 in the location of our proposed cluster. These authors argued that there is no clear red sequence of galaxies associated with this structure. However, we have shown in the i vs $i-K_s$ plot of Fig. 3 that indeed there is a red sequence of galaxies suggestive of a cluster and as we can see in Fig. 4 that the galaxy density profile is also typical of a cluster. The existence of potential substructures deserve further investigation as it may indicate the cluster is in the process of formation.

3.1 Morphology

We discuss in the following paragraph the optical/near infrared morphological appearance of the galaxies with confirmed spectroscopic redshift in the GCl J0332.2-2752 cluster. In Fig. 5 we show the available ACS and VLT-ISAAC images for these galaxies. The six EROs look very compact and regular in the VLT-ISAAC images, nevertheless ID3698 has a double bulge and spiral arms in the ACS images, perhaps due to merging or cannibalism, and ID3920 is an AGN. The other four EROs are visually classified as E/S0 systems. ID3586 is an SBb or SBc galaxy which is merging with the small galaxy ID3656 (left up in the ACS images). ID3185 is too faint to be classified but it would be an Sa or Sb system, the galaxy which is up in the images has a higher photometric redshift. The last object ID2859 is also too faint to be classified but look like a spiral galaxy, up in the images there is a galaxy with a higher photometric redshift.

3.2 X-Ray data

We use the X-ray images of the CDF-S in order to detect possible diffuse or extended emission from the GCl J0332.2-2752 cluster of galaxies (Rosati, et al. 2002b). No X-ray extended sources have been found in the region where the cluster is located (Giacconi et al. 2002). We work with the image of the soft band (0.5-2.0 keV events) taken from the CDF-S web page [3]. In Fig. 6 left we show the VLT-K_s image of the cluster of galaxies with overlaid Chandra X-ray contours, data are from the 0.5-2.0 keV events smoothed with a 5 arcsec FWHM Gaussian. Here we can see the X-ray emission from the AGN is weakly extended towards the brightest galaxy in the cluster. Now we evaluate the net counts in the 0.5-2.0 keV band in a 35 arcsec aperture of the X-ray emission centred in the optical centroid of the

[3] http://www.mpe.mpg.de/~mainieri/cdfs_pub/index.html

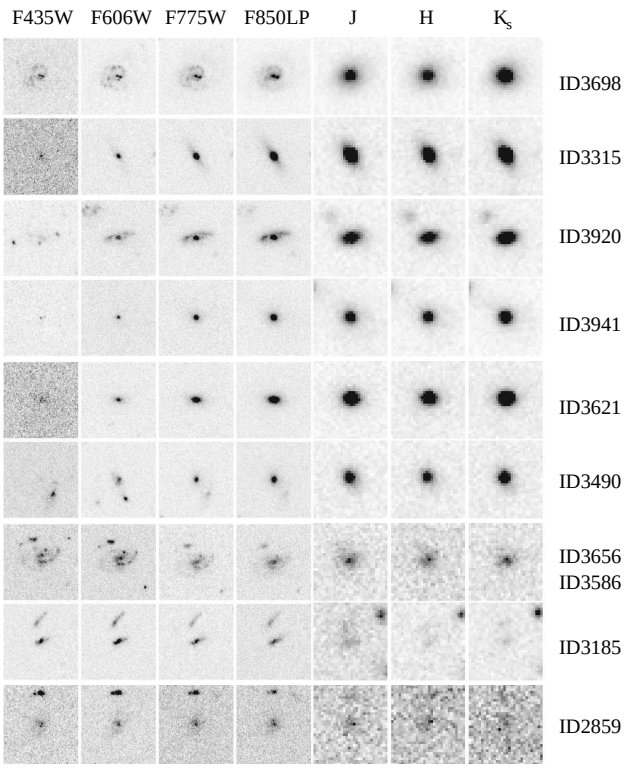

Figure 5. Multiband ACS and VLT-ISAAC image of the galaxies belonging to the GCl J0332.2-2752 cluster of galaxies. Each ACS image is 3.6 arcsec on a side and each VLT-ISAAC image is 4.5 arcsec on a side.

cluster. We take a 35 arcsec aperture in order to compare with the low luminosity clusters in Stanford et al. (2001). We find 1067 counts with an effective exposure time of 777 ks (calculated from the exposure map given in Giacconi et al. (2002)). The background was estimated locally using three source-free circular apertures (r=10 arcsec) located around the cluster. The background corrected counts in the r=35 arcsec aperture was 319 ± 30 which corresponds to a flux of $(1.9 \pm 0.2) \times 10^{-15}$ erg cm^{-2} s^{-1} and a rest frame luminosity of $L_X = (1.6 \pm 0.2) \times 10^{43}$ erg s^{-1} (0.5-2.0 keV).

In order to study a possible underlying extended source we subtract the point-spread function (PSF) of the brightest sources near to the core cluster from the soft band X-ray smoothed image. The result is plotted in Fig. 6 right

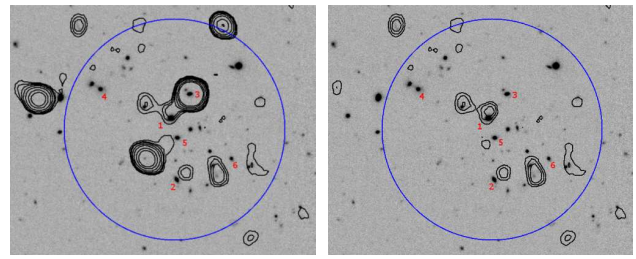

Figure 6. Left: Chandra contours of X-ray emission (0.5-2.0 keV) in GCl J0332.2-2752 overlaid on the VLT-K_s image. The Chandra data are smoothed with a 5 arcsec FWHM Gaussian. Contours correspond to $[2, 3, 5, 7, 15, 25, 50]\sigma$ above the local background. The blue circle has a radius of 35 arcsec and it is approximately centred in the position of the optical cluster. Right: the same but after applying a PSF subtraction of the brightest sources. The EROs members of the cluster are marked in both figures by a number from the brightest to lowest luminosity EROs (1 is the brightest) in the K_s band. 1 is ID3698, 2 (ID3315), 3 (ID3920), 4 (ID3941), 5 (ID3619), and 6 (ID3490).

which shows the VLT-K_s image with the X-ray contours from the PSF subtracted X-ray image. The residual X-ray contours are located close but do not coincide precisely with the positions of galaxies. The centre of the X-ray emission within the 35 arcsec aperture (denoted in the figure as a blue circle), was calculated as the flux-weighted centroid of all events in this image and agrees well with the optical centre of the cluster. Nevertheless since there is no obvious extended emission, using the PSF subtracted X-ray image, we simply evaluate the flux in the aperture by integrating all the counts. After correction for background, it results 153 ± 30 net counts which leads to an upper limit to the possible X-ray flux emission in the band of $(9 \pm 2) \times 10^{-16}$ erg cm^{-2} s^{-1}. This flux corresponds to a rest frame luminosity of $L_X = (6.0 \pm 1.3) \times 10^{42}$ erg s^{-1}. Thus, we limit the X-ray luminosity of the cluster to less than $L_X = 7.3 \times 10^{42}$ erg s^{-1} (0.5-2.0 keV). Such low value is consistent with expectations from the $L_X - \sigma_v$ relationship (Mulchaey 2000). GCl J0332.2-2752 is the less luminous high redshift ($z > 1$) galaxy cluster found so far (see e.g. Bremer et al. (2006); Stanford et al. (2001)).

4 CONCLUSIONS

We have used a cluster-finding algorithm based in the clustering of EROs at a given photometric redshift in order to find high redshift galaxy clusters in the GOODS-MUSIC dataset. We identify a cluster of distant galaxies, GCl J0332.2-2752, at $z = 1.10$ in the GOODS Southern Field. Nine galaxies present spectroscopic redshift in the range of $1.094 < z_{\rm spec} < 1.101$ and within 50 arcsec (0.42 Mpc) from the brightest infrared galaxy. Six of them are EROs and lie within a radius of 24 arcsec (0.20 Mpc) from this galaxy. The velocity dispersion of the GCl J0332.2-2752 cluster of galaxies along the line-of-sight is $\sigma_v = 433^{+152}_{-74}$ km s^{-1} which corresponds to the Abell richness class $R = 0$, virial radius $R_{200} = 0.6^{+0.2}_{-0.1}$ Mpc, mass $M_{\rm cl} = 4.9^{+1.6}_{-0.8} \times 10^{13} M_\odot$ and intracluster gas temperature $k_B T \sim 1.5$ KeV. We limit the X-ray luminosity of the cluster to less than $L_X = 7.3 \times 10^{42}$

erg s^{-1} (0.5-2.0 keV). This upper limit is consistent with the value predicted from the local $L_X - \sigma_v$ relation.

This is one of the lower mass clusters found to date at redshift $z > 1$. Such clusters will be hard to find with any other method: in X-ray it is difficult even with very deep exposures; they may be out of reach for the upcoming generation of Sunyaev-Zeldovich surveys; using weak lensing techniques it is very complicated to detect clusters at these low masses even with deep HST observations (detection of groups was achieved via stacking of shear signals). Thus, beside studying the environment of high-z radio sources, deep optical/near infrared surveys appear as a valid alternative to study the population of low-mass galaxy clusters at $z > 1$.

ACKNOWLEDGMENTS

This work was supported by Project No. 03065/PI/05 from the Fundación Séneca and Plan Nacional de Astronomía y Astrofísica Project AYA2005-06543. We acknowledge to the ESO/GOODS and the Chandra Deep Field projects and the teams that carried out programs LP168.A-0485 and LP170.A-0788 with the Very Large Telescope at the ESO Paranal Observatory.

REFERENCES

Adami, C., Mazure, A., Ilbert, O., et al. 2005, A&A, 443, 805
Blanton, E.L., Gregg, M.D., Becker, R.H., and White, R.L., 2003, AJ, 125, 1635
Bartelmann, M., 1996, A&A, 313, 697
Best, P.N., 2000, NMRAS, 317, 720
Bremer, M.N., Valtchanov, I., Willis, J. et al. 2006, NMRAS, 371, 1427
Butcher, H., and Oemler, A.Jr., 1984, ApJ, 285, 426
Capozziello, S., and Cardone, V.F., 2004, Phys. Rev. D, 70, 123501
Cimatti, A., Daddi, E., Mignoli, M., et al., 2002, A&A, 381, L68
Cimatti,A., Daddi, E., Cassata, P., et al., 2003, A&A, 412, L1
Danese, L., De Zotti, G., and di Tullio, G., 1980, A&A, 82, 322
Finn, R.A., Zaritsky, D., McCarthy, D.W., et al., 2005, ApJ, 630, 206
Frenk, C.S., Evrard, A.E., White, S.D.M., and Summers, FlJ., 1996, ApJ, 472, 460
Giacconi, R., Zirm, A., Wang, J., et al., 2002, ApJS, 139, 369
Gilli, R., 2004, MSAIS, 5, 301
Grazian, A., Fontana, A., de Santis, C., et al., 2006, A&A, 449, 951
Hansen, S.M., Mckay, T.A., Wechsler, R.H., et al., 2005, ApJ , 633, 122
Jing, Y.P, 2000, AJ, 535, 30
LeFevre, O., Vettolani, G., Paltani, S., et al., 2004, A&A, 428, 1043
Lubin, L.M. and Bahcall, N.A., 1993, ApJ, 415, L17
Mignoli, M., Cimatti, A., Zamorani, G., et al., 2005, A&A, 437, 883
Mulchaey, J.S., 2000, ARA&A, 38, 289
Mullis, C.R., Rosati, P., Lamer, G., et al., 2005, ApJ, 623, L85
Munshi, D., Porciani, C., and Wang, Y., 2004, MNRAS, 349, 281
Moustakas, L.A., Casertano, S., Conselice, C.J., et al., 2004, ApJ, 600, L131
Nakata, F., Kajisawa, M., Yamada,T., et al., 2001, PASJ, 53, 1139
Navarro, J.F., Frenk, C.S., and White, S.D.M., 1993, MNRAS, 53, 1139
Pointecouteau, E., Arnaud, M., and Pratt G.W., 2005, A&A, 435, 1
Rosati, P., Borgani, S., and Norman, C., 2002a, ARA&A, 40, 539.
Rosati, P., Tozzi, P., Giacconi, R., et al., 2002b, ApJ, 566, 667.
Szokoly, G.P., Bergeron, J., Hasinger, G., et al., 2004, ApJS, 155, 271
Stanford, S.A., Elston, R., Eisenhardt, P.R., et al., 1997, AJ, 114, 2232
Stanford, S.A., Holden, B., Rosati, P., et al., 2001, ApJ, 552, 504
Stanford, S.A., Eisenhardt, P.R., Brodwin, M., et al., 2005, ApJ, 634, L129
Stanford, S.A., Romer, A.K., Sabirli, K., et al., 2006, ApJ, 646, L13
Szokoly, G.P., Bergeron, J., Hasinger, G., et al., 2004, ApJS, 155, 271
Tomotsugu, G., Sadanori, O., Massafumi, Y., et al., 2003, PASJ, 55, 739
Vanzella, E., Cristiani, S., Dickinson, M., et al., 2005, A&A, 434, 53
Vanzella, E., Cristiani, S., Dickinson, M., et al., 2006, A&A, 454, 423
Voit, G.M., 2005, RvMP, 77, 207
Wolf, C., Meisenheimer, K., Roser, H.J., et al., 2001, A&A, 365, 681
Yee, H.K.C., and Ellingson, E., 2003, ApJ, 585, 215

This paper has been typeset from a TEX/ LATEX file prepared by the author.